

# Some phenomenological consequences of the time-ordered perturbation theory of QED on noncommutative spacetime

Yi Liao, Christoph Dehne

Institut für Theoretische Physik, Universität Leipzig,  
Augustusplatz 10/11, D-04109 Leipzig, Germany

## Abstract

A framework was recently proposed for doing perturbation theory on noncommutative (NC) spacetime. It preserves the unitarity of  $S$  matrix and differs from the naive, popular approach already at the lowest order in perturbation when time does not commute with space. In this work, we investigate its phenomenological implications at linear colliders, especially the TESLA at DESY, through the processes of  $e^+e^- \rightarrow \mu^+\mu^-$ ,  $H^+H^-$ ,  $H^0H^0$ . The results are indeed found to be very different from the ones obtained in the naive approach. The first two get corrected at tree level as opposed to the null result in the naive approach, while the third one coincides with the naive result only in the low energy limit. The impact of the Earth rotation is incorporated. The NC signals are generally significant when the NC scale is comparable to the collider energy. If this is not the case, the nontrivial azimuthal angle distribution and day-night asymmetry of events due to Lorentz violation and the Earth rotation will be useful in identifying signals. We also comment briefly on the high energy behaviour of the cross section that grows up linearly in the center of mass energy squared and argue that it does not necessarily contradict some statements, e.g., the Froissart-Martin bound, achieved in ordinary theory.

PACS: 11.10.Nx, 13.40.-f, 14.80. Cp

Keywords: noncommutative field theory, linear collider

# 1 Introduction

Field theory on noncommutative (NC) spacetime has stimulated a lot of investigations since it was found to arise naturally in the context of string theory [1]. A possible way to formulate a field theory on NC spacetime is to implement the Weyl-Moyal correspondence that replaces in the action the usual product of field operators by their star product,

$$(f_1 \star f_2)(x) = \left[ \exp \left( \frac{i}{2} \theta^{\mu\nu} \partial_\mu^x \partial_\nu^y \right) f_1(x) f_2(y) \right]_{y=x}. \quad (1)$$

Here  $x, y$  are the usual commutative coordinates and  $\theta_{\mu\nu}$  is a real, antisymmetric, constant matrix characterizing the noncommutativity of spacetime,  $[\hat{x}_\mu, \hat{x}_\nu] = i\theta_{\mu\nu}$ . The  $\theta$  parameter has the dimension of length squared and is presumably related to some energy scale  $\Lambda_{\text{NC}}$  where NC physics sets in. Considering the connection of NC field theory to string theory and that gravity may be unified with gauge interactions in the string framework at a TeV scale [2], it seems reasonable to expect that  $\Lambda_{\text{NC}}$  should be not far above a TeV. This possibility opened an avenue to extensive phenomenological studies that could test the ideas of NC physics in low or high energy experiments[3]-[7]. Concerning these, we mention one point which will be relevant to our present work. Since  $\theta_{\mu\nu}$  is a constant matrix instead of a Lorentz tensor, Lorentz invariance is explicitly broken in NC field theory. As pointed out in Ref. [3], this has important repercussions on data analysis of collider experiments done on the Earth which rotates by itself and revolves around the Sun. In Ref. [4], it has been shown how this seemingly troublesome problem can be used as an advantage in discriminating NC signals from those in the ordinary commutative theories like the standard model and other new physics. It has also been argued that for collider experiments on the Earth the main impact comes from the relative change of the directions of  $\theta_{\mu\nu}$  to the locally fixed reference frame as the Earth rotates. This apparent change of directions has been further elaborated upon recently in Ref. [5]. We shall continue to include this effect in the present work.

All of perturbative calculations performed so far in NC field theory have been based on the understanding that the only difference of NC theory from its commutative counterpart is the appearance of NC phases in Feynman rules of interaction vertices [8, 9]. It was found however that such a perturbation framework cannot preserve the unitarity of  $S$  matrix when time does not commute with space, i.e.,  $\theta_{0i} \neq 0$  [10]. This may be understood as follows. A typical NC phase looks like  $\exp(i/2 \theta_{\mu\nu} p^\mu k^\nu)$  where  $p, k$  are the momenta of the relevant particles. When it appears in a loop diagram, one of the momenta will represent

the loop momentum to be integrated over. For  $\theta_{0i} \neq 0$ , the zero-th component of the loop momentum enters into the phase. Then we cannot arbitrarily Wick rotate it to the imaginary axis since there is no guarantee any more that the integrand vanishes rapidly enough at infinity in the complex plane. In such a case, the imaginary part of a forward scattering amplitude will get additional contributions from the NC phase. This is in sharp contradiction to the unitarity relation which states that the imaginary part can only be associated with physical thresholds which in turn are determined by internal propagators independently of vertices. This failure in unitarity may not be necessarily attributed to the noncommutativity of time and space, but may well be due to the improper perturbation framework instead. Indeed, as demonstrated for the one-loop self-energy in  $\varphi^3$  theory in Ref. [11] (see also Ref. [12]), the approach using the Yang-Feldman equation gives a unitary result that is consistent with the general considerations in Ref. [13]. More recently, starting from some basic assumptions concerning perturbation theory that are commonly adopted in the literature, it has been shown [14] (see also [15]) that a careful treatment of the time-ordering procedure does not lead to the naive formalism as first formulated in Ref. [8] when  $\theta_{0i} \neq 0$ . Instead, it results in a framework which is the old-fashioned, time-ordered perturbation theory (TOPT) modified properly to the NC context. Unitarity can be preserved as long as the interaction Lagrangian is explicitly Hermitian. More importantly, the new framework differs from the old one already at tree level although the two become identical when  $\theta_{0i} = 0$ . The whole picture of perturbation theory is thus altered for the case of  $\theta_{0i} \neq 0$ .

In the present work we shall start to pursue the phenomenological consequences of the new perturbation framework. We shall work out the simplest processes at linear colliders that feel NC effects,  $e^+e^- \rightarrow \mu^+\mu^-, H^+H^-, H^0H^0$ . Here  $H^\pm, H^0$  could be any scalars that participate in NC scalar QED interactions although they will be considered as Higgs bosons in our mind. We shall find in the next section that the results are indeed very different from those obtained in the naive approach. In the latter approach, there are no corrections at tree level to the first two processes, and the third one was computed in Ref. [4]. However, in TOPT the first two also get corrected and the third one approaches the naive result only in the low energy limit. More surprisingly, when the process occurs in the  $s$  channel through a massless intermediate state, the NC corrected term in the cross section can grow up linearly in  $s$ , the center of mass energy squared. We shall argue in the last section how this does not necessarily contradict the Froissart-Martin bound

obtained in ordinary field theory. Our numerical analysis including the Earth rotation effect is detailed in section 3, and our results are summarized in the last section.

## 2 Calculation of the processes

We present the analytic part of our calculation in this section. We first review the time-ordered perturbation theory adapted for NC field theory in Ref. [14]. This is then followed by calculation of cross sections in the local reference frame fixed to a particular collider. The Earth rotation effects are included in the last subsection.

### 2.1 Computational rules

Ref. [14] starts with some basic assumptions about perturbation theory on NC spacetime that are usually made in the literature. The Green functions are defined in terms of vacuum expectation values of the time-ordered products of field operators and the exponentiated interaction action. The usual time-ordering procedure is adopted and the free theory is taken to be a good starting point for perturbation theory. It has then been shown that, when  $\theta_{0i} \neq 0$  the resulting perturbation framework is not the naive, seemingly covariant one as extensively used in the literature [8, 9], but the old-fashioned, time-ordered perturbation theory extended with new NC interaction vertices. The two formalisms coincide when time commutes with space, but are not equivalent in the opposite case especially concerning the fate of unitarity. In the language of TOPT, a physical process is virtualized as a series of transitions between physical intermediate states that are sequential in time. The unitarity of  $S$  matrix is thus apparent if the interaction Lagrangian is explicitly Hermitian. Actually, as shown there, unitarity holds valid for generally off-shell Green functions as well. In the following we shall list the computational rules for NC vertices to be used here which are part of the prescriptions spelled out in Ref. [14]. We refer the interested reader to that reference for a detailed exposition.

For our purpose, the Lagrangian for spinor and scalar QED on NC spacetime is given by,

$$\begin{aligned}
\mathcal{L} = & -\frac{1}{4}F^{\mu\nu} \star F_{\mu\nu} + \bar{\psi} \star (\gamma^\mu iD_\mu - m)\psi \\
& + \frac{1}{2}(D_\mu\varphi_0) \star (D^\mu\varphi_0) - \frac{1}{2}m_0^2\varphi_0 \star \varphi_0 \\
& + (D_\mu\varphi)^\dagger \star (D^\mu\varphi) - m_\pm^2\varphi^\dagger \star \varphi.
\end{aligned} \tag{2}$$

Here  $\psi$  is the charged spinor field ( $e^-$  or  $\mu^-$ ) with mass  $m$ ,  $\varphi$  and  $\varphi_0$  are the charged

( $H^-$ ) and neutral ( $H^0$ ) scalar fields with mass  $m_{\pm}$  and  $m_0$  respectively.  $A$  is the electromagnetic field with coupling  $e$ . The covariant derivatives and field tensor are defined by the generalized gauge invariance,

$$\begin{aligned}
F_{\mu\nu} &= \partial_{\mu}A_{\nu} - \partial_{\nu}A_{\mu} + ie[A_{\mu}, A_{\nu}]_{\star}, \\
D_{\mu}\varphi_0 &= \partial_{\mu}\varphi_0 + ie[A_{\mu}, \varphi_0]_{\star}, \\
D_{\mu}\varphi &= \partial_{\mu}\varphi + ieA_{\mu} \star \varphi, \\
D_{\mu}\psi &= \partial_{\mu}\psi + ieA_{\mu} \star \psi,
\end{aligned} \tag{3}$$

where  $[A, B]_{\star} = A \star B - B \star A$  is the Moyal bracket. The processes to be considered here also occur through weak interactions in the standard model, so in principle we should include the NC modifications for this part. Since the attempts to generalize the standard model to NC spacetime have not been successful so far [16], we shall not try to guess what the modified weak interactions would look like. In this sense, our calculations should be considered as NC corrections to QED results.

For the processes here, we only need the rules for the vertices  $A\bar{\psi}\psi$ ,  $A\varphi^{\dagger}\varphi$  and  $A\varphi_0\varphi_0$ , which are found to be,

$$\begin{aligned}
\bar{\psi}(p_2, \lambda_2)\psi(p_1, \lambda_1)A^{\mu}(p_3, \lambda_3) &= +e\gamma^{\mu}P_{231}, \\
\varphi^{+}(p_2, \lambda_2)\varphi(p_1, \lambda_1)A^{\mu}(p_3, \lambda_3) &= +e(p_{1\lambda_1} - p_{2\lambda_2})^{\mu}P_{231}, \\
\varphi^0(p_2, \lambda_2)\varphi^0(p_1, \lambda_1)A^{\mu}(p_3, \lambda_3) &= -e/2[p_{1\lambda_1}^{\mu}(P_{132} - P_{231} + P_{321} - P_{123}) \\
&\quad + p_{2\lambda_2}^{\mu}(P_{231} - P_{132} + P_{312} - P_{213})],
\end{aligned} \tag{4}$$

where the NC phase  $P_{jkl} = \exp[-i(p_{j\lambda_j}, p_{k\lambda_k}, p_{l\lambda_l})]$  with  $(a, b, c) = a \wedge b + b \wedge c + a \wedge c$  and  $a \wedge b = 1/2 \theta_{\mu\nu}a^{\mu}b^{\nu}$ . All momenta are meant to be incoming. The parameter  $\lambda$  denotes the direction of time flow along the momentum direction, which is  $+$ ( $-$ ) if the vertex is the later (earlier) end of the line.  $p_{\lambda}^{\mu} = (\lambda E_{\mathbf{p}}, \mathbf{p})$  with  $E_{\mathbf{p}} = \sqrt{\mathbf{p}^2 + \mu^2}$  denotes the on-shell four-momentum with positive or negative energy of a particle with mass  $\mu$  and three-momentum  $\mathbf{p}$ . It should be noted that only on-shell momenta are involved in the vertices. This is indeed in the spirit of TOPT which treats all intermediate states as physical ones. The point here, as emphasized in Ref. [14] is that, the seemingly covariant formalism which treats intermediate states as off-shell cannot be recovered as in ordinary theory when  $\theta_{0i} \neq 0$ . This will also be verified in our following calculations.

## 2.2 Cross sections in the locally fixed reference frame

Let us first compute the process of  $e^+e^- \rightarrow \mu^+\mu^-$ . Its time-ordered Feynman diagrams are shown in Fig. 1, where the wavy and arrowed solid lines stand for the photon and  $e^-$  (or  $\mu^-$ ) fields respectively. The other arrows indicate momenta and the  $\lambda$  parameters of the

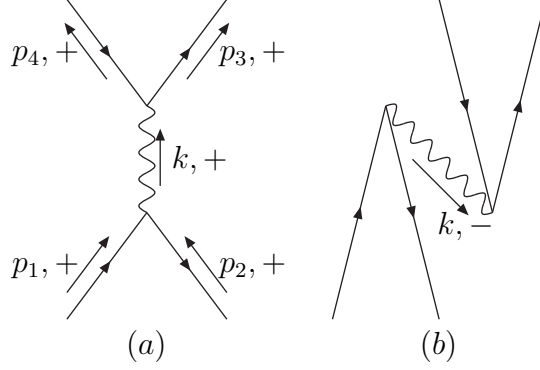


Figure 1: Time-ordered diagrams for  $e^+e^- \rightarrow \mu^+\mu^-$ . Time flows upwards.

time flow. For on-shell scattering we have  $\lambda_j = +$  for all external particles ( $j = 1, 2, 3, 4$ ) while  $\lambda = +, -$  corresponds to the two possible time-flows of the intermediate photon shown in Fig. 1(a) and 1(b).

Using the prescriptions in Ref. [14] and the above rules for vertices, the sum of the two diagrams is,

$$\begin{aligned}
& \bar{v}_2 e \gamma_\mu u_1 \bar{u}_3 e \gamma^\mu v_4 (-2\pi) \delta(E_1 + E_2 - E_3 - E_4) \sum_\lambda \int \frac{d^3 \mathbf{k}}{(2\pi)^3 2\omega_{\mathbf{k}}} \\
& \times (2\pi)^3 \delta^3(\mathbf{p}_1 + \mathbf{p}_2 - \mathbf{k})^3 (2\pi)^3 \delta^3(\mathbf{k} - \mathbf{p}_3 - \mathbf{p}_4)^3 (-1) [\lambda(E_1 + E_2) - \omega_{\mathbf{k}} + i\epsilon]^{-1} \\
& \times \exp[-i(p_{2\lambda_2}, -k_\lambda, p_{1\lambda_1})] \exp[-i(-p_{3\lambda_3}, k_\lambda, -p_{4\lambda_4})],
\end{aligned} \tag{5}$$

where  $E_j$ 's are the external particles energies and  $\omega_{\mathbf{k}} = |\mathbf{k}|$  is the energy of the intermediate photon. Note that there is an extra minus sign for the energy deficit factor for the photon intermediate state compared to the scalar one. Finishing the phase space integral and dropping the global four-momentum conservation factor, we obtain the transition amplitude as

$$\begin{aligned}
\mathcal{A} &= \bar{v}_2 e \gamma_\mu u_1 \bar{u}_3 e \gamma^\mu v_4 (2\omega_{\mathbf{k}})^{-1} \sum_\lambda [\lambda(E_1 + E_2) - \omega_{\mathbf{k}} + i\epsilon]^{-1} \\
&\times \exp[-i(p_{2+}, -k_\lambda, p_{1+})] \exp[-i(p_{3+}, -k_\lambda, p_{4+})],
\end{aligned} \tag{6}$$

with  $k = p_1 + p_2 = p_3 + p_4$ . The plus sign subscripts to  $p_j$ 's may be dropped since they are already on-shell four-momenta of positive energy. We keep them to emphasize the point that, generally,  $p_{1\lambda_1} + p_{2\lambda_2} \neq k_\lambda \neq p_{3\lambda_3} + p_{4\lambda_4}$ .

When  $\theta_{0i} = 0$ , all  $\lambda$  parameters are automatically removed from the NC phases. Then the  $\lambda$  dependence resides exclusively in the energy deficit factor. The NC phases may be

simplified using the four-momentum conservation, e.g.,  $\exp[-i(p_2, -k, p_1)] = \exp[-ip_1 \wedge p_2]$ . The sum over  $\lambda$  is finished using,

$$\frac{1}{2\omega_{\mathbf{k}}} \sum_{\lambda} \frac{1}{\lambda(E_1 + E_2) - \omega_{\mathbf{k}} + i\epsilon} = \frac{1}{k^2 + i\epsilon}. \quad (7)$$

We thus reproduce the result that would have been obtained in the naive approach,

$$\mathcal{A} = \bar{v}_2 e\gamma_{\mu} u_1 \bar{u}_3 e\gamma^{\mu} v_4 \frac{e^{-ip_1 \wedge p_2} e^{-ip_4 \wedge p_3}}{k^2 + i\epsilon}, \text{ for } \theta_{0i} = 0, \quad (8)$$

which deviates from the QED result by a global phase only and thus gives the same cross section.

For  $\theta_{0i} \neq 0$  however, the  $\lambda$  dependence remains in NC phases. Denoting  $n^{\mu} = (0, \hat{\mathbf{k}})$  so that  $k_{\lambda}^{\mu} = \lambda\omega_{\mathbf{k}}(1, \vec{0}) + \omega_{\mathbf{k}}n^{\mu}$ , we have for any momentum  $q$ ,  $k_{\lambda} \wedge q = \omega_{\mathbf{k}}(1/2 \lambda\theta_{0i}q^i + n \wedge q)$ . The NC phases in eq. (6) become,

$$\exp[-i(p_2 \wedge p_1 + p_3 \wedge p_4 + \omega_{\mathbf{k}}n \wedge q)] \exp[-i\lambda\omega_{\mathbf{k}}\theta_{0j}q^j/2], \quad (9)$$

with  $q = p_2 + p_3 - p_1 - p_4$ . The sum over  $\lambda$  in eq. (6) can be finished using

$$\frac{1}{2\omega_{\mathbf{k}}} \sum_{\lambda} \frac{\exp[-i\lambda a]}{\lambda(E_1 + E_2) - \omega_{\mathbf{k}} + i\epsilon} = \frac{1}{k^2 + i\epsilon} \left[ \cos a - i(E_1 + E_2) \frac{\sin a}{\omega_{\mathbf{k}}} \right], \quad (10)$$

with  $a = \omega_{\mathbf{k}}\theta_{0j}q^j/2$ . Note that in contrast to the case of  $\theta_{0j} = 0$ , the NC phases for the two time-flows do not factorize any more; instead, they interfere to produce a new imaginary part. Then,

$$\begin{aligned} \mathcal{A} &= \exp[-i(p_2 \wedge p_1 + p_3 \wedge p_4 + \omega_{\mathbf{k}}n \wedge q)] \bar{v}_2 e\gamma_{\mu} u_1 \bar{u}_3 e\gamma^{\mu} v_4 \\ &\times \frac{1}{k^2 + i\epsilon} \left[ \cos a - i(E_1 + E_2) \frac{\sin a}{\omega_{\mathbf{k}}} \right]. \end{aligned} \quad (11)$$

Now we specialize to the center of mass frame (c.m.) fixed locally to a particular collider. Then,  $\mathbf{k}, \omega_{\mathbf{k}} \rightarrow 0$  so that

$$\begin{aligned} \mathcal{A} &= \exp[-i(p_2 \wedge p_1 + p_3 \wedge p_4)] \bar{v}_2 e\gamma_{\mu} u_1 \bar{u}_3 e\gamma^{\mu} v_4 \\ &\times \frac{1}{k^2 + i\epsilon} \left[ 1 - i\frac{1}{2}(E_1 + E_2)\theta_{0j}q^j \right] \\ &= \exp[-i(p_2 \wedge p_1 + p_3 \wedge p_4)] \bar{v}_2 e\gamma_{\mu} u_1 \bar{u}_3 e\gamma^{\mu} v_4 \\ &\times s^{-1} \left[ 1 + i\theta_{0j}(p_1 - p_3)^j \sqrt{s} \right], \text{ in c.m. ,} \end{aligned} \quad (12)$$

where  $s$  is the c.m. energy squared. The unpolarized differential cross section is found to be,

$$\frac{d\sigma^{\mu}}{d\Omega} = \frac{\alpha^2}{4s} (1 + c_{\theta}^2) f^{\mu}, \quad (13)$$

where  $c_\theta = \cos \theta$ ,  $s_\theta = \sin \theta$  etc with  $\theta, \varphi$  being the polar and azimuthal angles of  $\mu^-$  in the local reference frame. (This  $\theta$  should not be confused with the NC parameter.)  $f^\mu$  is the NC correction factor,

$$f^\mu = 1 + \frac{1}{4} \left( \frac{\sqrt{s}}{\Lambda_{\text{NC}}} \right)^4 (w_i - w_f)^2, \quad (14)$$

where we have defined the NC parameter vector  $\theta_E^j = \theta_E^{0j}$ , with  $\Lambda_{\text{NC}} = |\vec{\theta}_E|^{-1/2}$  being the associated NC energy scale, and  $w_i = \hat{\theta}_E \cdot \hat{\mathbf{p}}_1$ ,  $w_f = \hat{\theta}_E \cdot \hat{\mathbf{p}}_3$  using the relevant unit vectors. We have also ignored the masses of the electron and muon which is appropriate for high energy collisions. Note that the NC correction term in  $f^\mu$  grows up as  $s^2$ . Since we did not make any low energy approximations, it holds true at high energies as long as the NC QED persists to be a valid description of QED interactions on NC spacetime. This phenomenon arises due to the balance of the two competing factors. While the exchange of a soft, massless and on-shell photon in the center of mass tends to blow up the amplitude, the opposite but small NC phases from the two time-flows tend to annihilate the contributions. We shall discuss in the last section how this high energy behaviour does not necessarily contradict the Froissart-Martin bound derived in ordinary theory. Here we just comment that it implies a lower bound on the differential cross section,

$$\frac{d\sigma^\mu}{d\Omega} \geq \frac{\alpha^2}{4\Lambda_{\text{NC}}^2} (1 + c_\theta^2) |w_i - w_f|. \quad (15)$$

The  $H^+(p_4)H^-(p_3)$  production is similarly computed. Using the same notation as above, we find,

$$\begin{aligned} \mathcal{A} &= \exp[-i(p_2 \wedge p_1 + p_3 \wedge p_4 + \omega_{\mathbf{k}} n \wedge q)] e^2 \bar{v}_2(\not{p}_3 - \not{p}_4) u_1 \\ &\times \frac{1}{k^2 + i\epsilon} \left[ \cos a - i(E_1 + E_2) \frac{\sin a}{\omega_{\mathbf{k}}} \right], \end{aligned} \quad (16)$$

which again reduces to the standard QED result up to a global phase as in the naive approach when  $\theta_{0j} = 0$ . For  $\theta_{0j} \neq 0$  however, the second term also contributes. In the c.m., we have,

$$\begin{aligned} \mathcal{A} &= \exp[-i(p_2 \wedge p_1 + p_3 \wedge p_4)] e^2 \bar{v}_2 2\not{p}_3 u_1 \\ &\times s^{-1} \left[ 1 + i\theta_{0j} (p_1 - p_3)^j \sqrt{s} \right], \\ \frac{d\sigma^{H^\pm}}{d\Omega} &= \frac{\alpha^2}{8s} \beta_\pm^3 s_\theta^2 f^{H^\pm}, \end{aligned} \quad (17)$$

where  $\beta_\pm = \sqrt{1 - 4m_\pm^2/s}$  is the final particle velocity and,

$$f^{H^\pm} = 1 + \frac{1}{4} \left( \frac{\sqrt{s}}{\Lambda_{\text{NC}}} \right)^4 (w_i - \beta w_f)^2. \quad (18)$$



The  $H^0(p_3)H^0(p_4)$  process also occurs at tree level through an  $s$ -channel exchange of photon in NC QED. Its computation is slightly more complicated but straightforward. Finishing the trivial intermediate state phase space integral, we obtain,

$$\mathcal{A} = \frac{1}{2}e^2\bar{v}_2\not{p}_3u_1e^{-ip_2\wedge p_1}\sum_{\lambda}\frac{g(k_{\lambda})}{2\omega_{\mathbf{k}}[\lambda(E_1+E_2)-\omega_{\mathbf{k}}+i\epsilon]}, \quad (19)$$

where

$$g(k_{\lambda}) = e^{-ip_3\wedge p_4}\left[2e^{i2\omega_{\mathbf{k}}n\wedge(p_1-p_3)}e^{i\lambda\omega_{\mathbf{k}}\theta_{0j}(p_1-p_3)^j}\right. \\ \left.-e^{-i2\omega_{\mathbf{k}}n\wedge p_2}e^{-i\lambda\omega_{\mathbf{k}}\theta_{0j}p_2^j}-e^{i2\omega_{\mathbf{k}}n\wedge p_1}e^{i\lambda\omega_{\mathbf{k}}\theta_{0j}p_1^j}\right] \\ -(p_3\leftrightarrow p_4). \quad (20)$$

Note that  $\mathcal{A}$  is symmetric in  $p_3$  and  $p_4$  since the spinor part is antisymmetric as is  $g(k_{\lambda})$ . The summation over  $\lambda$  can be finished as in eq. (10), which is essentially,

$$\sum_{\lambda}\frac{g(k_{\lambda})}{2\omega_{\mathbf{k}}[\lambda(E_1+E_2)-\omega_{\mathbf{k}}+i\epsilon]} = \frac{1}{s}\left[\frac{1}{2}(g(k_+) + g(k_-)) + (E_1+E_2)\frac{g(k_+) - g(k_-)}{2\omega_{\mathbf{k}}}\right]. \quad (21)$$

For  $\theta_{0j} = 0$ , the above sum reduces to  $s^{-1}i8\sin(p_3\wedge p_4)$  so that

$$\mathcal{A} = i4e^2e^{ip_2\wedge p_1}\sin(p_3\wedge p_4)s^{-1}\bar{v}_2\not{p}_3u_1, \text{ for } \theta_{0j} = 0, \quad (22)$$

which is the result obtained in the naive approach [4]. The result for  $\theta_{0j} \neq 0$  is lengthy, so we specialize to the c.m.,

$$\mathcal{A} = -i2e^2e^{-ip_2\wedge p_1}\bar{v}_2\not{p}_3u_1s^{-1}(E_1+E_2)\theta_{0j}p_3^j\cos[(E_1+E_2)\theta_{0j}p_3^j/2], \quad (23)$$

which coincides with the naive one eq. (22) only to the leading order in the low energy limit. The differential cross section is

$$\frac{d\sigma^{H^0}}{d\Omega} = \frac{\alpha^2}{64}\frac{s}{\Lambda_{\text{NC}}^4}\beta_0^5s_{\theta}^2f^{H^0}, \quad (24) \\ f^{H^0} = \left[w_f\cos\left(\frac{s}{8\Lambda_{\text{NC}}^2}\beta_0w_f\right)\right]^2,$$

where now  $\beta_0 = \sqrt{1 - 4m_0^2/s}$ .

### 2.3 Earth rotation effects

The above results for cross sections would be the final ones to be used for data analysis if the collider were fixed relative to the reference frame in which  $\theta_{\mu\nu}$ 's are assigned values. This reference frame may be presumably defined by the microwave background radiation,

in which a collider fixed on the Earth is constantly moving due to the self-rotation of the Earth and its revolution around the Sun. Since a collider measurement takes much longer than a day to accumulate data, the motion of the Earth has to be taken into account in data analysis. As argued in Ref. [4], the dominant effect for a collider experiment comes from the relative change of the preferred directions defined by  $\theta_{\mu\nu}$  to our local terrestrial frame fixed by the geographic configuration of the considered collider. We shall include this effect in this subsection.

We first define the celestial and terrestrial reference frames. All frames are assumed to be right-handed and all azimuthal-like angles are measured counter-clockwise. The celestial frame may be fixed to good precision by specifying its 3-direction along the Earth's rotation axis and its 1-direction pointing to the vernal equinox [5]. The NC unit vector  $\hat{\theta}_E$  is then measured by the polar and azimuthal angles  $\rho \in [0, \pi]$  and  $\xi \in [0, 2\pi)$  which are NC physical parameters in addition to  $\Lambda_{\text{NC}}$ . For the local terrestrial frame, we define the  $e^-$  beam as the  $z$ -direction and the (outgoing) normal to the sphere of the Earth at the interaction point as the  $y$ -direction. The polar and azimuthal angles of a particle momentum in this frame are denoted as  $\theta \in [0, \pi]$  and  $\varphi \in [0, 2\pi)$  as in the last subsection. To consider the Earth rotation effect, we also have to know the geographic configuration of the collider which may be specified by three parameters. The site of the laboratory is determined by its latitude  $\sigma \in [-\pi/2, +\pi/2]$  with positive (negative) values denoting the northern (southern) hemisphere, and its longitude  $\omega \in [0, 2\pi)$  measured, e.g., with respect to the vernal equinox. We assume that the direction of the  $e^-$  beam deviates from the local meridian direction by an angle  $\delta \in [0, 2\pi)$ . The angles  $\sigma$  and  $\delta$  are fixed parameters for each collider, while  $\omega$  changes periodically as the Earth rotates.

The remaining task now is to express in the local frame the fixed unit vector  $\hat{\theta}_E$ , which is accomplished using the standard vector analysis [5],

$$\begin{aligned}\hat{\theta}_E^x &= s_\rho(c_{\omega-\xi}s_\sigma s_\delta + s_{\omega-\xi}c_\delta) - c_\rho c_\sigma s_\delta, \\ \hat{\theta}_E^y &= s_\rho c_{\omega-\xi} c_\sigma + c_\rho s_\sigma, \\ \hat{\theta}_E^z &= s_\rho(-c_{\omega-\xi}s_\sigma c_\delta + s_{\omega-\xi}s_\delta) + c_\rho c_\sigma c_\delta,\end{aligned}\tag{25}$$

where  $c_a = \cos a$ ,  $s_a = \sin a$  for all angles. In the following we shall denote  $\omega - \xi$  as  $\omega$  for simplicity. This means effectively that the angle  $\omega$  is measured with respect to the plane spanned by  $\hat{\theta}_E$  and the Earth rotation axis. Then, the quantities needed for cross sections

and defined in the last subsection are,

$$\begin{aligned} w_i &= \hat{\theta}_E^z, \\ w_f &= \hat{\theta}_E^x s_\theta c_\varphi + \hat{\theta}_E^y s_\theta s_\varphi + \hat{\theta}_E^z c_\theta. \end{aligned} \quad (26)$$

The Earth rotation effect enters through the apparent change of  $\hat{\theta}_E$  and thus cross sections.

### 3 Numerical results

Before we present our numerical results, let us summarize the sets of angles introduced so far: the local angles  $\theta$  and  $\varphi$ , the NC angular parameters  $\rho$  and  $\xi$ , the configuration angles  $\sigma$  and  $\delta$  of the collider, and the Earth rotation angle  $\omega$ . Since  $\xi$  appears in the combination of  $\omega - \xi$ , measuring  $\xi$  amounts to setting an absolute origin for  $\omega$  which may be chosen as the vernal equinox as mentioned above. In the following, our  $\omega$  will be measured with respect to  $\xi$  so that we shall concentrate on the single NC angle  $\rho$ . Our numerical results will be presented for the TESLA at DESY whose configuration angles are,  $\sigma = 53^\circ 34' 50''$ ,  $\delta = 27.5^\circ$  [17].

Upon considering the Earth rotation, the differential cross sections computed in the last section depend on the angles  $\theta, \varphi$  and  $\omega$  as well as others. We thus may have two types of distributions, one in the local angles, the other in the Earth rotation angle. The differential cross sections can be cast collectively in the form,

$$\frac{4\pi}{\sigma_0^A} \frac{d\sigma^A}{d\Omega} = F^A(\theta, \varphi; \omega), \quad A = \mu, H^\pm, H^0, \quad (27)$$

where  $\sigma_0^{\mu, H^\pm}$  are the standard QED total cross sections while  $\sigma_0^{H^0}$  is a convenient normalization constant for the  $H^0 H^0$  production,

$$\sigma_0^\mu = \frac{4\pi}{3} \frac{\alpha^2}{s}, \quad \sigma_0^{H^\pm} = \frac{\pi}{3} \frac{\alpha^2}{s} \beta_{\pm}^3, \quad \sigma_0^{H^0} = \frac{\pi \alpha^2}{60} \frac{s}{\Lambda_{\text{NC}}^4} \beta_0^5. \quad (28)$$

Then, in terms of  $f$  functions introduced in the last section, we have,

$$\begin{aligned} F^\mu(\theta, \varphi; \omega) &= \frac{3}{4}(1 + c_\theta^2) f^\mu, \\ F^{H^\pm}(\theta, \varphi; \omega) &= \frac{3}{2} s_\theta^2 f^{H^\pm}, \\ F^{H^0}(\theta, \varphi; \omega) &= \frac{15}{4} s_\theta^2 f^{H^0}. \end{aligned} \quad (29)$$

Let us first present the results of total cross sections or their ratios to the QED counterparts, which are averaged over the Earth rotation,

$$\bar{\sigma}^A = \sigma_0^A \bar{R}^A, \quad \bar{R}^A = \int \frac{d\omega}{2\pi} \int \frac{d\Omega}{4\pi} F^A(\theta, \varphi; \omega). \quad (30)$$

For the  $\mu^+\mu^-$  and  $H^+H^-$  processes the integrals can be finished but the results are too tedious to be recorded here. In Fig. 2 we show  $\bar{R}^\mu$  as a function of  $\sqrt{s}$  for different values of  $\Lambda_{\text{NC}}$  and  $\rho$ . The NC corrections are always positive and depend strongly on  $\Lambda_{\text{NC}}$  as it is clear from the form factor  $f^\mu$ . The  $\rho$  dependence is relatively much milder. Fig. 3 displays  $\bar{R}^{H^\pm}$  as a function of mass for the chosen parameters. From these two plots it is clear that the viability to detect NC deviations from QED in total cross sections will be decisively determined by the relative order of magnitudes of  $\Lambda_{\text{NC}}$  and  $\sqrt{s}$ . In this respect, the  $H^0$  pair production shown in Fig. 4 is more advantageous [4] since it occurs in the standard model at one loop. For comparable  $\Lambda_{\text{NC}}$  and  $\sqrt{s}$ , e.g.,  $\Lambda_{\text{NC}} = \sqrt{s} = 1$  TeV, the NC QED induced cross section well exceeds the one in the standard model which is about  $0.1 \sim 0.2$  fb for an intermediate mass  $H^0$  [18].

The normalized and averaged distributions in the local angles shown in Figs. 5 and 6 are defined as,

$$\begin{aligned} F^A(\theta) &= \int \frac{d\omega}{2\pi} \int \frac{d\varphi}{2\pi} F^A(\theta, \varphi; \omega), \\ F^A(\varphi) &= \int \frac{d\omega}{2\pi} \frac{1}{2} \int d\cos\theta F^A(\theta, \varphi; \omega). \end{aligned} \quad (31)$$

Again, for comparable  $\Lambda_{\text{NC}}$  and  $\sqrt{s}$ , there are sizable NC deviations in  $\theta$  dependence from the QED results for the  $\mu^+\mu^-$  and  $H^+H^-$  production or from the standard model result for the  $H^0H^0$  production which follows roughly the  $\sim \sin^2\theta$  law [18]. More interesting are the  $\varphi$  distributions shown in Fig. 6, which occurs due to the violation of Lorentz invariance. The distributions are also more sensitive to the  $\rho$  parameter compared to other quantities shown above.

The above results are obtained by time-averaging and thus correspond to the standard data analysis for the collider measurement. But the novel feature of Lorentz violation can be better displayed using the day-night asymmetry [4], which describes the impact of the Earth rotation and is defined as a function of  $\omega$  ( $\pi$ ) or  $t = 12\omega/\pi$  (hour),

$$\begin{aligned} A_{\text{DN}}^A(\omega_a, \omega_b) &= \frac{\left[ \int_{\omega_a}^{\omega_b} d\omega - \int_{\omega_a+\pi}^{\omega_b+\pi} d\omega \right] \sigma^A(\omega)}{\left[ \int_{\omega_a}^{\omega_b} d\omega + \int_{\omega_a+\pi}^{\omega_b+\pi} d\omega \right] \sigma^A(\omega)} \\ &= \frac{\left[ \int_{\omega_a}^{\omega_b} d\omega - \int_{\omega_a+\pi}^{\omega_b+\pi} d\omega \right] \int \frac{d\Omega}{4\pi} F^A(\theta, \varphi; \omega)}{\left[ \int_{\omega_a}^{\omega_b} d\omega + \int_{\omega_a+\pi}^{\omega_b+\pi} d\omega \right] \int \frac{d\Omega}{4\pi} F^A(\theta, \varphi; \omega)}. \end{aligned} \quad (32)$$

The asymmetry is shown in Fig. 7 as histograms binned per half an hour for the  $H^+H^-$  and  $H^0H^0$  production for the same set of parameters as in Fig. 5. The overall asymmetries

accumulated for 24 hours are respectively,  $A_{\text{DN}}^{H^\pm}(0, \pi) = +2.74 \times 10^{-2}$  and  $A_{\text{DN}}^{H^0}(0, \pi) = -9.18 \times 10^{-2}$ . This asymmetry and the azimuthal angle distribution are the most sensitive probe to NC signals and its angular parameter  $\rho$ .

## 4 Conclusion and discussion

The naive approach of perturbative NC field theory [8, 9] was shown to lead to the violation of unitarity when time does not commute with space [10]. This failure has been attributed to the improper implementation of perturbation theory [11]. Recently, it has been demonstrated that the usual assumptions about perturbation theory when handled properly actually result in an old-fashioned, time-ordered perturbation theory modified appropriately to include effects of NC spacetime [14]. It turns out that this framework does not recover the naive one when time does not commute with space, and that it preserves unitarity as long as the Lagrangian is explicitly Hermitian. The picture for perturbation theory is thus altered; in particular, the difference appears already at the first order in perturbation.

In the present work we investigated the phenomenological implications of the above framework at a high energy linear collider. We worked out the processes of  $e^+e^- \rightarrow \mu^+\mu^-, H^+H^-, H^0H^0$  and included the effects of the Earth rotation. The results are indeed found to be very different from those obtained in the naive approach. The first two processes get corrected already at tree level as opposed to the naive result that amplitudes are only modified by a global phase and thus cross sections remain untouched. For the third process, the results in the two approaches are also different although they coincide in the low energy limit. The numerical significance of NC effects depends on the geographic configuration of the collider as well as the basic NC parameters. For definiteness, we presented our numerical results for the TESLA project. Generally speaking, the new effects are significant when the NC energy scale is comparable to the collider energy. When this is not the case, the relatively rare signals can be compensated for by their unique characteristics due to Lorentz violation, as shown in the azimuthal distribution and day-night asymmetry of events.

Finally, we comment briefly on the surprising result on the high energy behaviour of cross section. We found in section 2 that the NC correction term in the total cross section grows up linearly in  $s$  when a soft, massless, on-shell photon is exchanged in the  $s$ -channel.

Actually the phenomenon occurs when the mass of the exchanged particle is much less than the NC energy scale and  $s$ . We argue below that this does not necessarily contradict the statements in ordinary theory. For example, the Froissart-Martin bound that the cross section of two body reactions cannot grow faster than  $\ln^2 s$  as  $s \rightarrow \infty$ , was originally obtained [19] on the assumption of the Mandelstam's representation [20], i.e., the double dispersion relation. Later this bound was derived [21] from the usual axioms of quantum field theory based on the analyticity properties of scattering amplitudes, in particular causality and relativistic invariance. In NC field theory, these last properties are already changed even with space-space noncommutativity alone: only a weaker microcausality is possible in the sense of perturbation theory at least and a part of Lorentz invariance survives [22]. The analyticity properties are altered so significantly that no dispersion relations have been shown to be possible for the simplest case of scattering [22], let alone the double dispersion relations of Mandelstam. As the time-space NC is generally believed to be more delicate than the space-space NC, it is far from obvious that the Froissart-Martin bound would still apply to the time-space NC case. Another statement that is often made in ordinary theory is that unitarity sets a bound on the total cross section in the high energy limit. This is not a precise statement in fact. Indeed, unitarity of the  $S$  matrix sets a bound on each of the partial wave cross sections, but it is insufficient to do so on the total cross section which is an infinite sum of the partial wave cross sections [23]. Only when a process is known to occur for a finite number of partial waves in the high energy limit, a bound becomes possible on the total cross section. As there are preferred directions in NC field theory, this partial wave analysis would be very different but seems to deserve further study.

**Acknowledgements** We thank K. Sibold for helpful discussions and carefully reading the manuscript. Y.L. thanks P. M. Zerwas for communications about the TESLA project and M. Chaichian for clarifying comments and discussions about the Froissart-Martin bound and drawing Ref. [21] to his attention.

## References

- [1] A. Connes, M. R. Douglas, A. Schwarz, *Noncommutative geometry and matrix theory: compactification on tori*, J. High Energy Phys. 02(1998)003 [hep-th/9711162]; M. R. Douglas, C. Hull, *D-branes and the noncommutative torus*, *ibid.* 02(1998)008 [hep-th/9711165]; C.-S. Chu, P.-M. Ho, *Noncommutative open string and D-brane*, Nucl. Phys. B550(1999)151 [hep-th/9812219]; *Constrained quantization of open string in background B field and noncommutative D-brane*, *ibid.* B568(2000)447 [hep-th/9906192]; V. Schomerus, *D-branes and deformation quantization*, J. High Energy Phys. 06 (1999) 030 [hep-th/9903205]; N. Seiberg, E. Witten, *String theory and noncommutative geometry*, *ibid.* 09(1999)032 [hep-th/9908142].
- [2] N. Arkani-Hamed, S. Dimopoulos, G. Dvali, *The hierarchy problem and new dimensions at a millimeter*, Phys. Lett. B429(1998)263 [hep-ph/9803315]; *Phenomenology, astrophysics and cosmology of theories with submillimeter dimensions and TeV scale quantum gravity*, Phys. Rev. D59(1999)086004 [hep-ph/9807344]; I. Antoniadis, N. Arkani-Hamed, S. Dimopoulos, G. Dvali, *New dimensions at a millimeter to a fermi and superstrings at a TeV*, Phys. Lett. B436(1998)257 [hep-ph/9804398].
- [3] J. L. Hewett, F. J. Petriello, T. G. Rizzo, *Signals for noncommutative interactions at linear colliders*, Phys. Rev. D64(2001)075012 [hep-ph/0010354].
- [4] H. Grosse, Y. Liao, *Pair production of neutral Higgs bosons through noncommutative QED interactions at linear colliders*, Phys. Rev. D64(2001)115007 [hep-ph/0105090].
- [5] J. Kamoshita, *Probing noncommutative space-time in the laboratory frame*, hep-ph/0206223.
- [6] P. Mathews, *Compton scattering in noncommutative spacetime at the NLC*, Phys. Rev. D63(2001)075007 [hep-ph/0011332]; S. Baek, D. K. Ghosh, X.-G. He, W.-Y. P. Hwang, *Signatures of noncommutative QED at photon colliders*, *ibid.* D64(2001)056001 [hep-ph/0103068]; S. Godfrey, M.A. Doncheski, *Signals for noncommutative QED in  $e\gamma$  and  $\gamma\gamma$  collisions*, *ibid.* D65(2002)015005 [hep-ph/0108268]; C.E. Carlson, C.D. Carone, *Discerning noncommutative extra dimensions*, *ibid.* D65(2002)075007 [hep-ph/0112143]; T.M. Aliev, O. Ozcan, M. Savci, *The  $\gamma\gamma \rightarrow H^0 H^0$  decay in noncommutative quantum electrodynamics*, hep-ph/0209205.

- [7] I. Mocioiu, M. Pospelov, R. Roiban, *Low-energy limits on the antisymmetric tensor field background on the brane and on the noncommutativity scale*, Phys. Lett. B489(2000)390 [hep-ph/0005191]; M. Chaichian, M. M. Sheikh-Jabbari, A. Tureanu, *Hydrogen atom spectrum and the Lamb shift in noncommutative QED*, Phys. Rev. Lett. 86, 2716 (2001) [hep-th/0010175]; H. Grosse, Y. Liao, *Anomalous C violating three photon decay of the neutral pion in noncommutative quantum electrodynamics*, Phys. Lett. B520(2001)63 [hep-ph/0104260]; S.M. Carroll, *et al*, *Noncommutative field theory and Lorentz violation*, Phys. Rev. Lett. 87(2001)141601 [hep-th/0105082]; I. Mocioiu, M. Pospelov, R. Roiban, *Breaking CPT by mixed noncommutativity*, Phys. Rev. D65(2002)107702 [hep-ph/0108136]; C. E. Carlson, C.D. Carone, R.F. Lebed, *Supersymmetric noncommutative QED and Lorentz violation*, hep-ph/0209077.
- [8] T. Filk, *Divergences in a field theory on quantum space*, Phys. Lett. B376(1996)53.
- [9] M. Chaichian, A. Demichev, P. Presnajder, *Quantum field theory on noncommutative space-times and the persistence of ultraviolet divergences*, Nucl. Phys. B567(2000)360 [hep-th/9812180]; C.P. Martin, D. Sanchez-Ruiz, *The one loop UV divergent structure of U(1) Yang-Mills theory on noncommutative  $R^4$* , Phys. Rev. Lett. 83(1999)476 [hep-th/9903077]; S. Minwalla, M. V. Raamsdonk and N. Seiberg, *Noncommutative perturbative dynamics*, J. High Energy Phys. 02(2000)020 [hep-th/9912072]; M. Hayakawa, *Perturbative analysis on infrared aspects of noncommutative QED on  $R^4$* , Phys. Lett. B478(2000)394 [hep-th/9912094]; *Perturbative analysis on infrared and ultraviolet aspects of noncommutative QED on  $R^4$* , hep-th/9912167.
- [10] J. Gomis, T. Mehen, *Space-time noncommutative field theories and unitarity*, Nucl. Phys. B591(2000)265 [hep-th/0005129].
- [11] D. Bahns, S. Doplicher, K. Fredenhagen, G. Piacitelli, *On the unitarity problem in space-time noncommutative theories*, Phys. Lett. B533(2002)178 [hep-th/0201222].
- [12] C. Rim, J. H. Yee, *Unitarity in space-time noncommutative field theories*, hep-th/0205193.
- [13] S. Doplicher, K. Fredenhagen, J. E. Roberts, *The quantum structure of spacetime at the Planck scale and quantum fields*, Commun. Math. Phys. 172(1995)187.



- [14] Y. Liao, K. Sibold, *Time-ordered perturbation theory on noncommutative spacetime: basic rules*, Eur. Phys. J. C25(2002)469 [hep-th/0205269]; *Time-ordered perturbation theory on noncommutative spacetime II: unitarity*, Eur. Phys. J. C25(2002)479 [hep-th/0206011].
- [15] H. Bozkaya, *et al*, *Space-time noncommutative field theories and causality*, hep-th/0209253.
- [16] For a recent comprehensive discussion, see for example: M. Chaichian, P. Presnajder, M. M. Sheikh-Jabbari, A. Tureanu, *Noncommutative gauge field theories: a no-go theorem*, Phys. Lett. B526 (2002) 132 [hep-th/0107037]; *Noncommutative standard model: model building*, hep-th/0107055. For discussions on the unitarity problem in the latter work, see: J. L. Hewett, F. J. Petriello, T. G. Rizzo, *Noncommutativity and unitarity violation in gauge boson scattering*, Phys. Rev. D66(2002)036001 [hep-ph/0112003].
- [17] P. M. Zerwas, private communication.
- [18] K. J. F. Gaemers, F. Hoogeveen, *Higgs boson pair production in  $e^+e^-$  reactions*, Z. Phys. C26(1984)249; A. Djouadi, V. Driesen, C. Junger, *Loop induced Higgs boson pair production at  $e^+e^-$  colliders*, Phys. Rev. D 54(1996)759 [hep-ph/9602341].
- [19] M. Froissart, *Asymptotic behaviour and subtractions in the Mandelstam representation*, Phys. Rev. 123(1961)1053.
- [20] S. Mandelstam, *Determination of the pion-nucleon scattering amplitude from dispersion relations and unitarity. General theory*, Phys. Rev. 112(1958)1344.
- [21] A. Martin, *Unitarity and high-energy behavior of scattering amplitudes*, Phys. Rev. 129(1963)1432.
- [22] Y. Liao, K. Sibold, *Spectral representation and dispersion relations in field theory on noncommutative space*, Phys. Lett. B549(2002)352 [hep-th/0209221].
- [23] See for example: R.G. Newton, *Scattering theory of waves and particles* (Springer-Verlag, 1982).

## Figure Captions

Fig. 2. The NC  $\mu^\pm$  cross section normalized to its QED counterpart is shown as a function of  $\sqrt{s}$  at the TESLA site. Other parameters are,  $\rho = 0$  (dotted),  $\pi/4$  (solid) and  $\pi/2$  (dashed) with  $\Lambda_{\text{NC}} = 1$  TeV, and  $\rho = \pi/4$  with  $\Lambda_{\text{NC}} = 4$  TeV (long-dashed).

Fig. 3. The NC  $H^\pm$  cross section normalized to its QED counterpart is shown as a function of its mass at the TESLA site and for  $\sqrt{s} = 0.5$  (dotted), 1.0 (solid) or 1.5 (dashed) TeV and  $\Lambda_{\text{NC}} = 1$  TeV,  $\rho = \pi/4$ .

Fig. 4. The NC  $H^0$  cross section is shown as a function of its mass using the same parameters as in Fig. 3.

Fig. 5. The normalized and averaged  $\theta$  distributions are shown for the NC processes (solid) and compared to their QED counterparts for  $\mu^\pm$  and  $H^\pm$  production (dashed).  $\rho = \pi/4$ ,  $\Lambda_{\text{NC}} = \sqrt{s} = 1$  TeV,  $m_\pm = m_0 = 150$  GeV.

Fig. 6. The normalized and averaged  $\varphi$  distributions are shown for  $H^\pm$  and  $H^0$  production at  $\rho = \pi/4$  (dashed) or  $\pi/3$  (solid). The case for  $\mu^\pm$  production is close to  $H^\pm$  and thus not shown. Other parameters are the same as in Fig. 5.

Fig. 7. The histograms of the day-night asymmetry  $A_{\text{DN}}$  are shown as a function of time  $t$  using the same parameters as in Fig. 5.

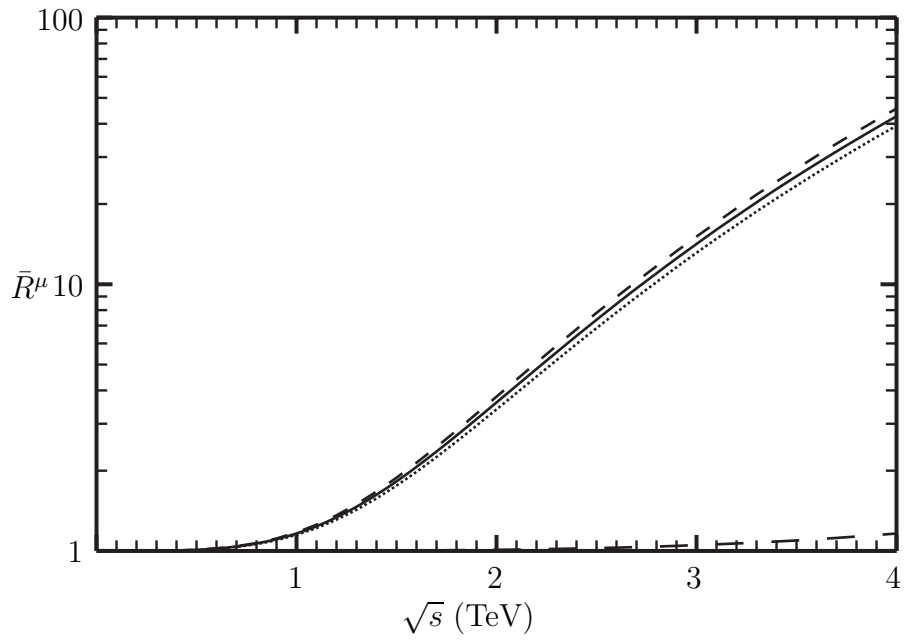


Figure 2

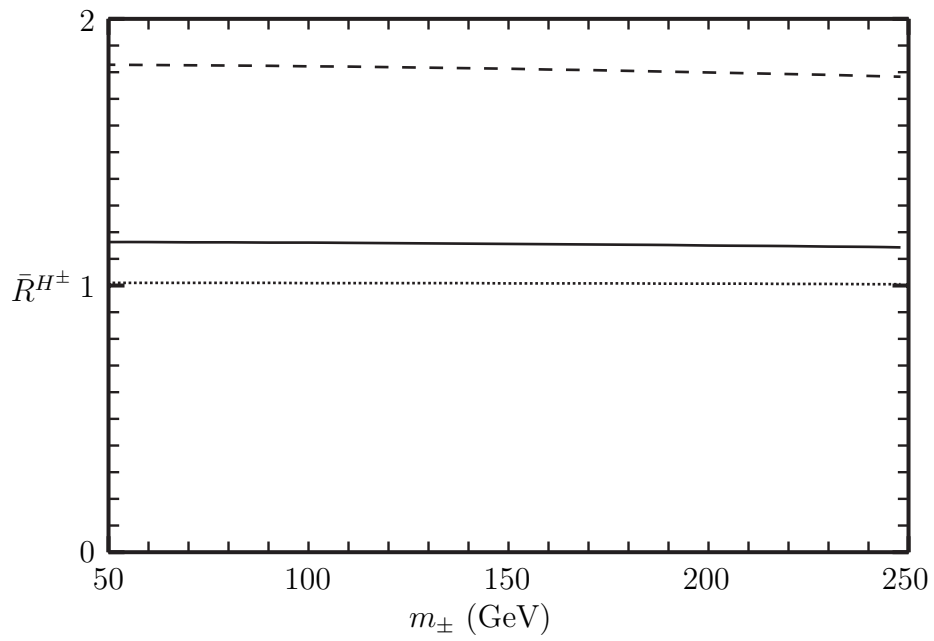


Figure 3

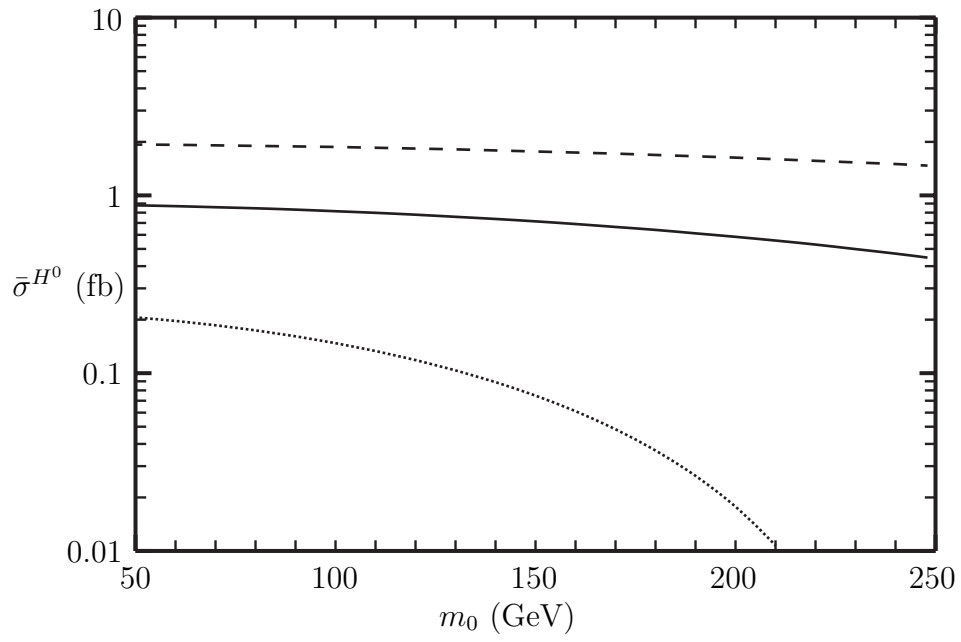


Figure 4

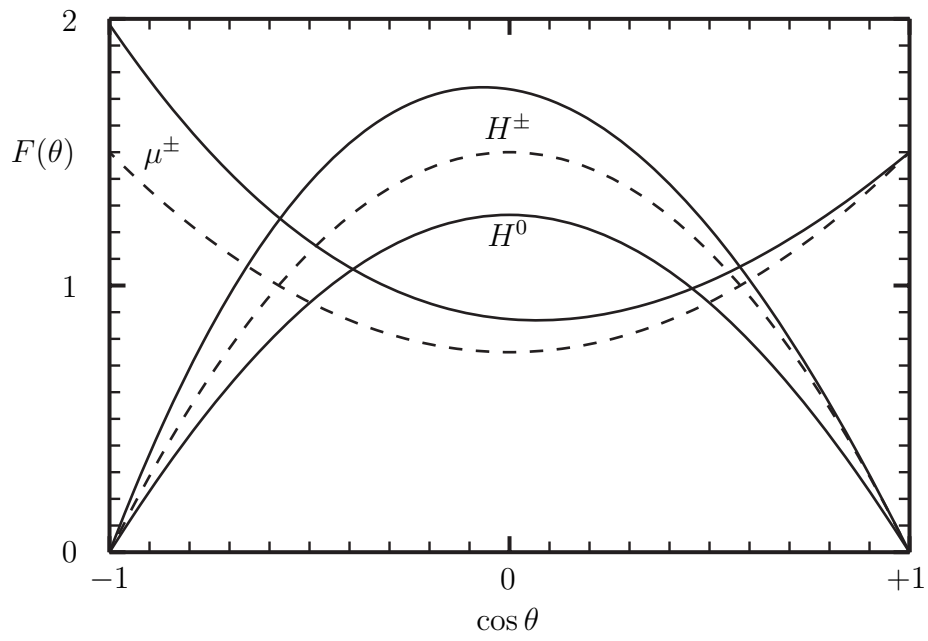


Figure 5

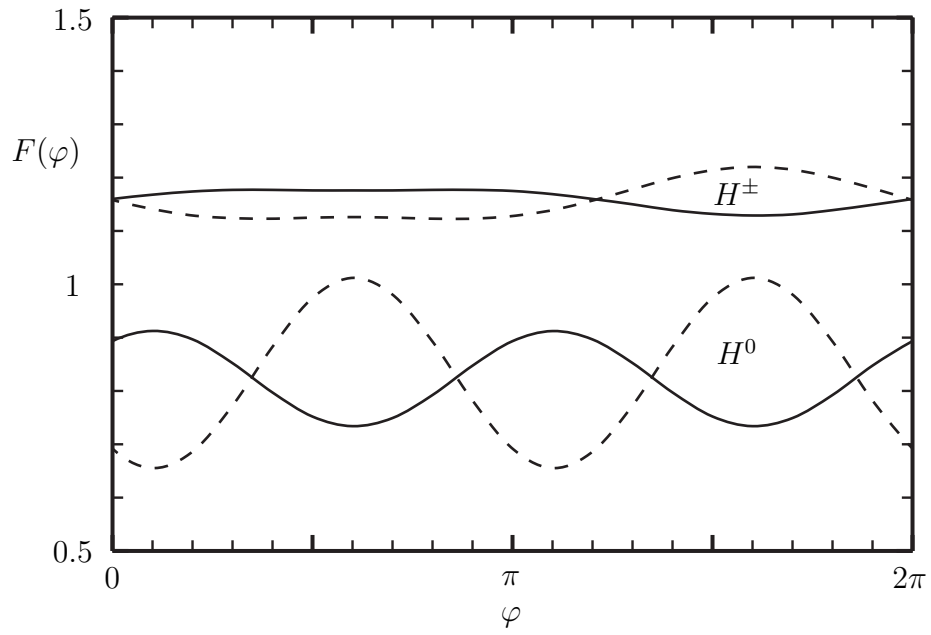


Figure 6

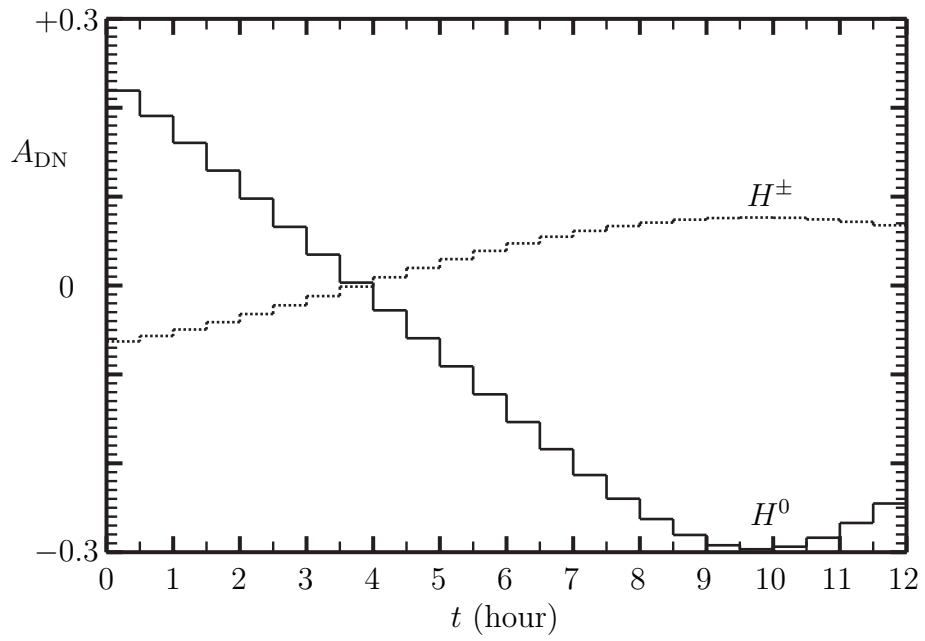


Figure 7